Food Chemistry: X 26 (2025) 102296

Contents lists available at ScienceDirect

Food Chemistry: X

journal homepage: www.sciencedirect.com/journal/food-chemistry-x

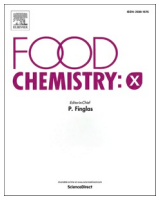

# Non-covalent interaction of sacha inchi protein and quercetin: Mechanism and physicochemical property

Tao Yang [a], Shanshan Li [a], Wenqin Su [a], Kun Pan [a,*], Fei Peng [b,*]

[a] School of Pharmacy, Engineering Research Center of Tropical Medicine Innovation and Transformation of Ministry of Education, Hainan Medical University, Haikou 571199, China
[b] School of Food Science and Engineering, Nanchang University, Nanchang, Jiangxi Province 330047, China

ARTICLE INFO

*Keywords:*
Non-covalent interaction
Sacha Inchi protein
Quercetin
Mechanism
Physicochemical property

ABSTRACT

Interactions between proteins and polyphenols are essential for the functional properties of foods. This study explores the non-covalent interactions between Sacha Inchi protein (SIP) and quercetin (Que) and examines the physicochemical characteristics of their complex. Fourier transform infrared spectroscopy and Circular dichroism indicated that Que could interact with SIP and change the secondary structure of SIP. The mechanism of Que binding significantly and quenching SIP fluorescence were revealed by fluorescence spectroscopy. The primary forces driving this interaction are hydrogen bonds and van der Waals forces. Additionally, binding with quercetin led to a marked increase in the β-sheet content of SIP and a decrease in random coil structures. With increasing Que levels, its loaded amount rose, although the encapsulation efficiency decreased. SIP-Que complexes displayed larger particle sizes and enhanced antioxidant properties than SIP alone, with antioxidant activity increasing with higher Que concentrations. Furthermore, the bioaccessibility of Que improved upon binding with SIP. This research contributes to the modification of SIP protein and its potential applications in the food industry.

## 1. Introduction

Sacha inchi, also known as Plukenetia Volubilis L., contains many essential amino acids in its protein, such as cysteine, tyrosine, threonine, and tryptophan (Wang et al., 2018). Sacha inchi protein (SIP) offers high nutritional value, even surpassing that of soybeans and peanuts. Despite this, research on SIP applications remains limited. Interactions between polyphenols and proteins can alter the physicochemical properties of proteins and enhance the bioavailability of polyphenolic compounds, thus increasing their nutritional value (Zhao et al., 2020). These interactions can lead to novel functional foods and materials. For instance, combining soybean protein with rutin improves emulsion stability due to rutin's role at the oil-water interface (Cui et al., 2014). Similarly, interactions between polyphenols and gluten proteins can reduce gluten allergies and inflammation, and create new biomaterials (Girard & Awika, 2020). Anthocyanins in grapes and blueberries form stable polyphenol particles through interactions with proteins, which maintain their stability during gastrointestinal transit without losing bioactivity (Xiong et al., 2020).

Quercetin (Que), a key flavonoid and polyphenolic compound found in fruits and vegetables such as celery, parsley, onions, and blueberries, is known for its antioxidant, anti-inflammatory, anticancer, and anti-aging properties (Zhang & Zhong, 2013). However, Que's chemical instability, low permeability, and bioaccessibility often lead to its degradation during digestion (Doosti et al., 2019). Binding Que with proteins can enhance its stability in liquid foods and improve its bioaccessibility. Polyphenol-protein interaction particles are emerging as effective carriers (Ghayour et al., 2019). Research shows that nanoparticles made of β-lactoglobulin and Que enhance the bioavailability of Que (Mirpoor et al., 2017). Additionally, the interaction between silk fibroin and quercetin has been found to synergistically boost the antioxidant properties of the material (Lozano-Pérez et al., 2017). Among the study of polyphenol-modified proteins, SIP has hardly been studied, in addition, Que and other nutrients are combined with protein and macromolecules to design a stable, safe, and highly soluble nutrient delivery system, which holds promise as a functional component in food development and formulation (Song et al., 2024). Sacha inchi as a national new resource food is less developed in China. Additionally, the combination of phenolic compounds with proteins leads to significant changes in structure and physicochemical properties and also broadens

* Corresponding authors.
*E-mail addresses:* pankun001219@163.com (K. Pan), pengf0129@foxmail.com (F. Peng).

https://doi.org/10.1016/j.fochx.2025.102296
Received 22 October 2024; Received in revised form 19 January 2025; Accepted 16 February 2025
Available online 19 February 2025

the application range of proteins (Vasava et al., 2022). Sacha inchi has a high protein content but lower application, so the study of its protein and Que can explore the properties of this protein and add new materials to the drug delivery system for solving the problem of low utilization of polyphenols. Thus, the combination of SIP and Que has high research value.

This study aims to clarify the non-covalent interactions between SIP and Que and explore the properties and biological activities of SIP-Que nanoparticles. Initially, the Fourier transform infrared spectroscopy (FTIR), fluorescence spectroscopy, and circular dichroism (CD) spectroscopy were used to examine the interaction between SIP and Que. Subsequently, the physicochemical properties and biological activities of the resulting complexes, including particle size, antioxidant activity, and Que bioaccessibility, were evaluated. This research provides insights into the phenolic modification and the potential applications of SIP in the food industry.

## 2. Materials and methods

### 2.1. Materials

SIP was obtained from a commercial company Hainan Hongke Biotechnology Co., LTD (Hainan, Haiko, China). Que with a purity of >95 % was procured from Shanghai Macklin Bio-Technology Co., Ltd. (Shanghai, China). Pepsin and trypsin were sourced from Aladdin Industrial Corporation (Shanghai, China). The reagent kits assessing antioxidant activity, including the scavenging capacity of DPPH free radicals, ABTS radicals, and hydroxyl radicals, were acquired from Nanjing Jiancheng Bioengineering Institute. All other reagents used in this study were commercially available.

### 2.2. Preparation of SIP solution ad SIP-Que complex solution

The preparation of the SIP solution was carried out according to the previously described method (Dai et al., 2022) with slight modifications. Briefly, SIP (5 g) was dissolved in distilled water (100 mL) and adjusted to pH 8.0 using a sodium hydroxide solution (1 M). The mixture was stirred at 400 rpm for 4 h at 30 °C, followed by hydrated overnight at 4 °C. The incubated SIP suspension was centrifuged at 8000 ×*g* for 10 min to obtain the SIP solution. The concentration of the SIP solution was determined using the drying method at 100 °C.

The prepared SIP solution was diluted with the appropriate amount of distilled water to 0.3 mg/mL. Subsequently, Que solution dissolved with ethanol to 5 μg/mL, then was diluted to 0.103, 0.155, 0.207, and 0.414 mmol/L. Finally, the different concentrations of Que solution were added to the SIP solution (*v*/v = 5:1) and stirred under aerobic conditions at room temperature for 2 h.

### 2.3. FTIR assay

The measurement method has been slightly modified as reported by Hao et al. (2022). Each group of samples was freeze-dried using the vacuum freeze-dryer (LGJ-1 A-50, Fourring Scientific Instrument, Beijing). The sample powder (1 mg) was mixed thoroughly with 200 mg of potassium bromide powder and pressed into a pellet. An FTIR spectrometer (Nicolet iS5, Thermo Fisher Scientific, MA) were used to measure the FTIR spectra with the range from 400 to 4000 $cm^{-1}$. The resolution was 4 $cm^{-1}$ and the scan number was 64. The KBr pellet served as the blank.

### 2.4. Fluorescence spectroscopy assay

The effect of quercetin on SIP fluorescence was analyzed using fluorescence spectroscopy. Different concentrations of quercetin ethanol solution were mixed with SIP solution at a 1:5 volume ratio to obtain various SIP-Que complexes. A Cary Eclipse fluorescence spectrophotometer (Agilent Technology, CA, USA) was used to record the fluorescence intensity of the SIP-Que complex under the following conditions: excitation wavelength 280 nm, scanning range 300–500 nm, scanning speed 600 nm/min, emission bandwidth 5 nm, and spectral scanning interval 1 nm. The solvent without samples was served as blank.

### 2.5. CD spectroscopy

The CD spectrum of SIP in the presence and absence of Que was recorded to evaluate the secondary structure change of the protein. A CD spectrometer (Bio-Logic MOS-450, Claix, France) was used to scan the absorbance of the SIP-Que complex solutions with the range from 190 nm to 250 nm at 25 °C. The rate is 100 nm/min and the spectral interval is 0.1 nm. Additionally, nitrogen was continuously charged during the experiment. The corrected CD spectra were analyzed using Dichroweb software (http://dichroweb.cryst.bbk.ac.uk/html/home.shtm).

### 2.6. Encapsulation efficiency (EE) and loading amount (LA) assays

Que amounts in the complexes were determined according to the previous report with slight modifications (Liu et al., 2022). In brief, the embedded Que was first extracted using ethanol solution (50 %). After that, the mixtures were centrifuged (8000 *g*, 10 min). The extraction of Que was repeated thrice. Finally, the Absorbance of the suspension at 374 nm was determined with an ultraviolet spectrophotometer (TU-1901, Purkinje GENERAL Instrument Ltd., China). The standard curve of absorbance and concentration was drawn with the Que standard solution. The encapsulation efficiency (EE) was defined as the ratio of the binding Que amount to the total Que amount. The loading amount (LA) was defined as the ratio of the binding Que amount to the SIP amount.

### 2.7. Particle size and zeta potential assays

Methods refer to previous reports and make some modifications (Zhang, Hou, et al., 2022). Particle size and zeta potential of SIP-Que complexes in solution at 25 °C were measured using a Malvern Zeta sizer (Malvern Instruments, UK). The particle size of the sample was measured at a backscatter detection angle of 173°.

### 2.8. Scanning electron microscope (SEM)

Samples with different concentrations of Que were transferred to a clean sample vial, and the water was removed by vacuum freezing-drying. The samples were gold-plated by MSP-2S magnetron ion sputtering before scanning, and then the ultrastructure of samples was observed using scanning electron microscopy (JSM-7900F, Tokyo, Japan) at an accelerating voltage of 5.0 kV. Digital images were collected and some representative ones were presented.

### 2.9. Antioxidant activity assay

The antioxidant activity of SIP-Que complex powders was measured using commercial kits according to their operating instructions. For DPPH radicals scavenging ability, the results were expressed as microgram/millimole of trolox equivalent per milligram of powders. One unit of hydroxyl radical (·OH) scavenging activity was defined as the SIP-Que complex amount that reduced 1 mmol/L hydrogen peroxide at 37 °C in 1 min (U/mL). FRAP is expressed as the concentration of the $FeSO_4$ standard solution (mM).

### 2.10. Bioaccessibility assay

The bioaccessibility of the binding Que was assessed following a modified version of a previously described method (Ferreira-Santos et al., 2024). In brief, 1 mL of the sample was mixed with simulated

gastric digestion fluid, which comprised 9 mL of phosphate-buffered saline (100 mM, pH 2.0) adjusted with 1 M HCl and porcine pepsin (2000 U/mL). This mixture was incubated for 1.5 h at 37 °C with agitation at 100 rpm. Next, 5 mL of this digested solution was transferred to a new simulated intestinal digestion fluid, containing 5 mL of phosphate-buffered saline (100 mM, pH 7.5), bile salts (0.3 %), and trypsin (100 U/mL), and incubated for 2 h at 37 °C with agitation at 100 rpm. The remaining Que was then extracted using a 75 % aqueous ethanol solution through ultrasound (100 % amplitude, 30 min) and measured. A standard control was prepared using a free Que solution for comparison. The bioaccessibility was calculated using the appropriate equation.

$$\text{Bioaccessibility (\%)} = \frac{\textit{amount of Que after digestion}}{\textit{amount of added Que in the system}} \times 100\%$$

### 2.11. Statistic analysis

All experiments were independently conducted in triple and data were shown as means ± standard deviation. Data was analyzed using Duncan's test for one-way analysis of variance at the significant level $p < 0.05$ using SPSS 26.0 (IBM Corp., Armonk, NY, USA). Graphics are drawn using origin 2021.

## 3. Results and discussion

### 3.1. FTIR

Fig. 1 presents the infrared spectra of SIP and SIP-Que complexes. All spectra display a broad peak within the range of 3700–3000 $cm^{-1}$, corresponding to the amide A band of the protein. This peak is primarily attributed to the N—H stretching vibrations of the amino acids, with O—H stretching vibrations also occurring in this region (Yadav et al., 2020). Upon non-covalent binding with Que, the amide A peak exhibits a slight shift from 3385 $cm^{-1}$ to 3384–3382 $cm^{-1}$. This shift suggests that Que interacts with the SIP through hydrogen bonding. Additionally, a sharp peak at 2980 $cm^{-1}$ was observed after interacting with Que. Similar observations reported a characteristic peak of Que at 2928 $cm^{-1}$ (Jiang et al., 2022). The amide I band of SIP, which is indicative of the secondary structure of proteins, shifted from 1651 $cm^{-1}$ to 1652 $cm^{-1}$ after binding with Que. Furthermore, the peak intensity of the amide II band at 1417 $cm^{-1}$ was enhanced. These changes imply that the C═O groups, N—H bonds, and C—N bonds of the amino acids in SIP are involved in interactions with Que (Cheng et al., 2023). In comparison to the spectra of SIP alone, the SIP-Que complex introduced new peaks at 1087, 1046, and 878 $cm^{-1}$. These results provide crucial evidence that Que has interacted with SIP and has been successfully incorporated into the SIP.

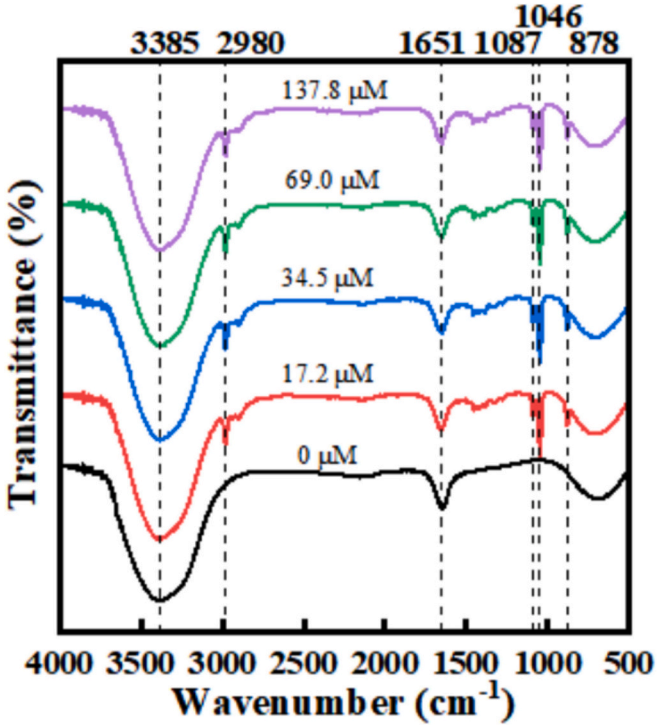


**Fig. 1.** FTIR spectrum of SPI and SIP-Que complexes.

### 3.2. Fluorescence spectroscopy

Fluorescence spectroscopy is extensively applied to investigate the interaction between small molecular ligands and proteins. We here detailly analyzed the interaction between quercetin and SIP using fluorescence spectroscopy. As depicted in Fig. 2, the fluorescence intensity of the SIP decreases gradually with the increment of Que concentration, and the maximum emission peaks were blue-shifted from 339 nm to 328 nm, indicating an obvious interaction between Que and the protein was present, resulting in the shielding of the indole groups of the amino acid residues (Günal-Köroğlu et al., 2022). This phenomenon also suggested the binding of Que to SIP resulted in a reduced polarity and enhanced hydrophobic environment for the amino acid residue (Zhang et al., 2023).

We applied the classical Stern-Volmer equation (Eq. 1) to investigate the fluorescence quenching of SIP induced by Que. Fig. 3A demonstrates a strong linear correlation between F0/F-1 and Que concentration across the tested temperatures. According to Table 1, the $K_{sv}$ value decreases with higher Que concentrations, while the $K_q$ value exceeds the maximum diffusion collision quenching constant ($2.0 \times 10^{10}$ L/mol/s). These findings indicate that the predominant quenching mechanism is dynamic quenching (Al-Shabib et al., 2018).

To further explore the binding characteristics, we analyzed the binding site number and binding constant using Eq. 2. Fig. 3B shows a linear relationship between log(F0-F/F) and log[Q]. As detailed in Table 1, the number of binding sites is approximately 1, suggesting that Que interacts with SIP through a single binding site. Furthermore, the Ka value decreases with rising temperature ($K_a = 4.83 \times 10^5$ L/mol (298.15 K); $4.26 \times 10^5$ L/mol (303.15 K); and $2.55 \times 10^5$ L/mol (310.15

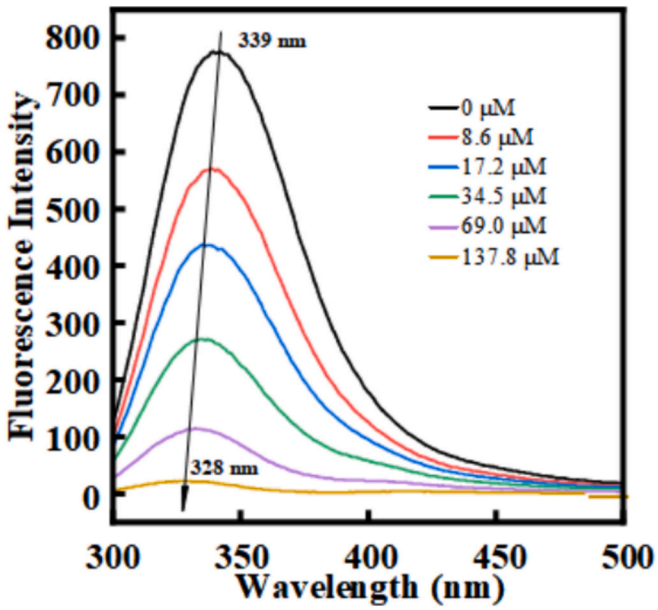


**Fig. 2.** The effect of Que concentration on the fluorescence intensity of SIP.

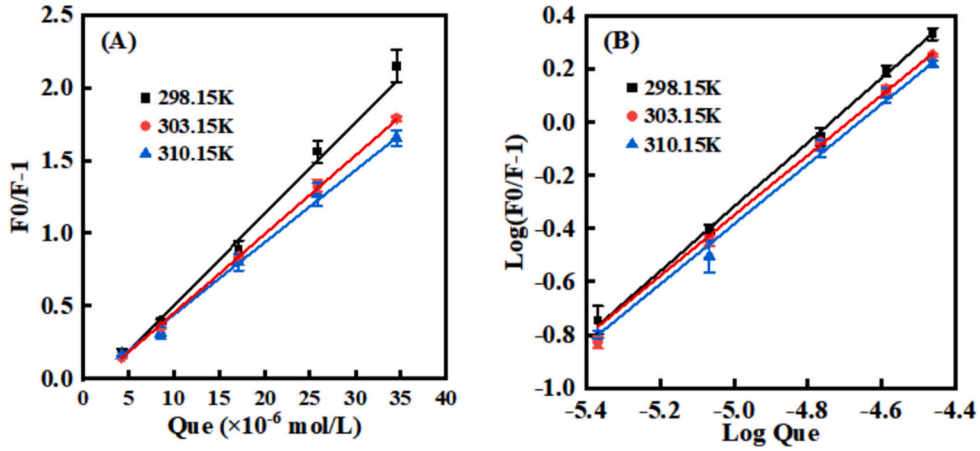


**Fig. 3.** Images of the fluorescence quenching of SIP by Que at different temperature based on Stern-Volmer equation. Que levels: 4.3, 8.6, 17.2, 25.8, 34.5 uM.

**Table 1**
Stern-Volmer constants and thermodynamic parameters of SIP-Que complexes at different temperature.

| Temperature (K) | Ksv (×10$^4$ L/mol) | n | Ka (×10$^5$ L/mol) | △G° (KJ/mol) | △H° (KJ/mol) | △S° (J/mol/K) |
|---|---|---|---|---|---|---|
| 298.15 | 6.61 | 1.20 | 4.83 | | | |
| 303.15 | 5.48 | 1.20 | 4.26 | −32.79 | −42.26 | −31.15 |
| 310.15 | 5.10 | 1.16 | 2.55 | | | |

K)). A highly protein-bound drug typically has a $K_a$ value between $10^5$ and $10^7$ L/mol, while a $K_a$ value between $10^2$ and $10^4$ L/mol indicates low to moderate binding strength (Hao et al., 2017). Thus, Que can bind to SIP *in vivo* with strong binding affinity.

$$\frac{F_0}{F} = 1 + K_{SV}[Q] = 1 + K_q\tau_0[Q] \quad (1)$$

$$lg\frac{F_0 - F}{F} = lgK_a + nlg[Q] \quad (2)$$

where F0 and F are the fluorescence intensity in the absence and presence of Que., respectively; $K_q$ and $\tau_0$ are the molecular quenching rate and fluorescence lifetime ($10^{-8}$ s), respectively; $K_a$ and n are the binding constant and the number of binding sites, respectively.

Non-covalent interactions between small and large molecules primarily involve electrostatic interactions, hydrogen bonds, van der Waals forces, and hydrophobic interactions. Using the Van't Hoff equations (Eqs. 3 and 4), we calculated thermodynamic parameters to characterize the non-covalent interaction between Que and SIP. Our findings indicate that both ΔG° and ΔH° values are negative, suggesting a spontaneous and exothermic binding process. Moreover, the negative values of ΔH° and ΔS° indicated that the binding process was mainly driven by enthalpy (Gan et al., 2024). In addition, they also implied that van der Waals forces and hydrogen bonds predominantly contribute to these interactions (Huang et al., 2020).

$$ln\Delta G^0 = -\frac{\Delta H^0}{RT} + \frac{\Delta S^0}{R} \quad (3)$$

$$\Delta G^0 = \Delta H^0 - T\Delta S^0 \quad (4)$$

where $\Delta G^0$, $\Delta H^0$, $\Delta S^0$ are the changes of Gibbs free energy, enthalpy, and entropy, respectively; T and R are the temperature and ideal gas constant, respectively.

### 3.3. CD spectroscopy

Circular dichroism spectroscopy is widely used for analyzing the secondary structure of proteins. Typically, α-helical structures are characterized by a positive peak at approximately 190 nm and a negative peak around 208 nm. β-sheet structures are associated with positive peaks near 195 nm and negative peaks around 215 nm, while random coil structures are characterized by a negative peak around 200 nm (Liu et al., 2021). Fig. 4 shows the changes in the circular dichroism spectra of SIP after binding with Que at various concentrations. Compared to SIP alone, SIP-Que complexes displayed a new positive peak at 200–203 nm and a negative peak at around 220 nm, indicating obvious alterations in β-sheet and random coil structures. Table 2 lists the relative contents of the secondary structure of SIP and SIP-Que complexes. Random coil is the predominant secondary structure of SIP, accounting for up to 70.45 %, possibly due to the acetic acid treatment during extraction. Visible changes in the secondary structure of SIP were observed after binding with Que. For instance, the β-sheet content increased from 13.35 % to 14.69–55.50 %, while the random coil decreased from 70.45 % to 14.10–28.47 %. The results suggest SIP folded upon the non-covalent bonding with Que, resulting in more compact structures (Zheng et al.,

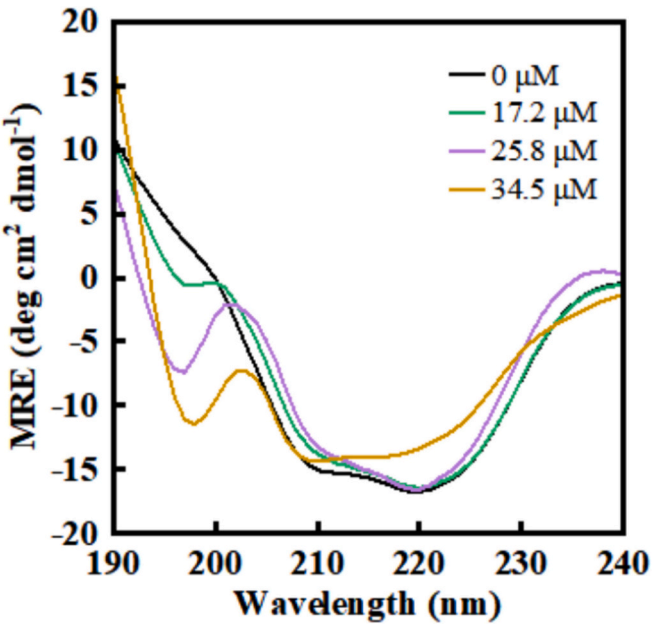


**Fig. 4.** CD images of SIP and SIP-Que complex.

**Table 2**
Secondary structure changes of SIP in the presence of Que.

| Entry | Que levels (μM) | α-helix | β-sheet | β-turn | Random coil |
|---|---|---|---|---|---|
| 1 | 0 | 7.45 % | 13.35 % | 8.70 % | 70.45 % |
| 2 | 17.2 | 43.90 % | 25.33 % | 5.40 % | 25.33 % |
| 3 | 25.8 | 4.47 % | 36.20 % | 44.43 % | 14.87 % |
| 4 | 34.5 | 5.65 % | 55.50 % | 24.75 % | 14.10 % |
| 5 | 69.0 | 10.83 % | 14.67 % | 46.03 % | 28.47 % |

2022). A similar phenomenon occurred in the binding of neohesperidin to ovalbumin (Xia et al., 2022). Neohesperidin, like Que, has hydrophobic groups and poor water solubility. In the presence of hydrophobic polyphenols, ovalbumin's conformation changes, with a decrease in α-helix and an increase in β-sheet.

### 3.4. EE and LA

Fig. 5 shows the variation in Que loading capacity and encapsulation efficiency at different SIP concentrations. Encapsulation efficiency decreases from 54.3 % at 17.2 μM to 27.7 % at 69 μM as Que concentration increases. Conversely, loading capacity shows an increasing trend, rising from 11.3 μg/mg to 23.1 μg/mg. Previous research has reported that the encapsulation efficiencies of quercetin bound non-covalently to almond protein and brown rice protein were below 20 % and 38 %, respectively (Kopjar et al., 2022). They also observed a decrease in encapsulation efficiency with increasing Que concentration, which is consistent with our findings. Additionally, Que bound to soy protein isolate through non-covalent interactions has shown encapsulation efficiencies ranging from 36 % to 86 %, indicating excellent loading capabilities (Zhang, Wang, et al., 2022). Compared with other carrier proteins, SIP has good quercetin-carrying capacity. Therefore, these results suggest SIP is a promising carrier for hydrophobic substances. Previous studies have shown that flavonoid structure influences protein binding affinity (Xia et al., 2022). The six hydroxyl groups on the glycosyl substituents at the C-7 position of the SIP carbon ring form hydrogen bonds with polar protein groups.

### 3.5. Particle size and zeta potential

As shown in Table 3, the particle sizes and zeta potentials of SIP-Que complexes at different Que concentrations. Compared to SIP alone, the

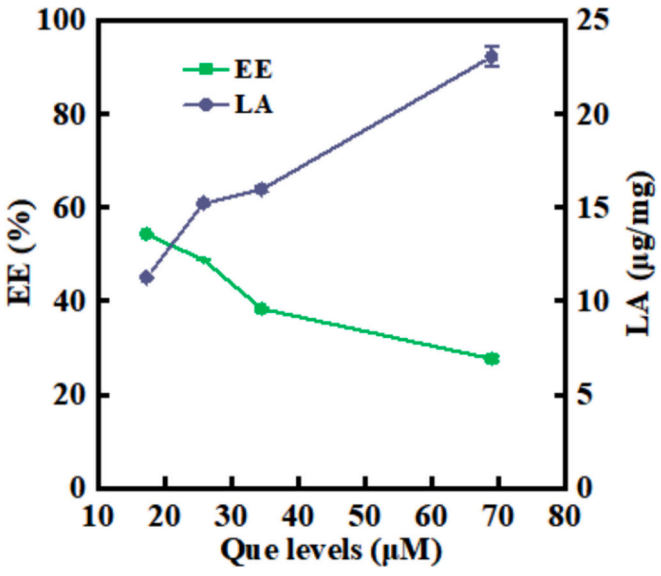


**Fig. 5.** The effect of Que levels on the EE and LA of Que in the SIP-Que complexes.

**Table 3**
Particle size and zeta potential of SIP-Que complexes prepared at different Que. concentration.

| Que. levels (μM) | 0 | 17.2 | 25.8 | 34.5 | 69.0 |
|---|---|---|---|---|---|
| Particle size (nm) | 163.8 ± 5.4 | 240.2 ± 8.8 | 199.4 ± 3.6 | 221.8 ± 4.0 | 302.5 ± 17.1 |
| Zeta potential (mV) | −23.86 ± 0.04 | −18.37 ± 0.03 | −21.47 ± 0.03 | −15.12 ± 0.03 | −20.83 ± 0.02 |

SIP-Que complexes showed a reduced negative charge (−21.47 mV to −15.12 mV *vs.* −23.86 mV), suggesting that the binding of Que diminished electrostatic repulsion between protein particles. A 'shield effect' from Que (neutral molecule), akin to the 'protein corona effect' on nanoparticle surfaces, may explain this phenomenon (Lozano-Pérez et al., 2017). Meanwhile, the complex particles are larger than the SIP. In particular, the average particle sizes of SIP-Que complexes were 1.85 times that of SIP alone at a Que level of 69.0 mM. Qie et al. (2021) reported that after binding with chlorogenic acid, the negative potential of β-lactoglobulin decreased while particle size increased, which was consistent with our findings. Thus, the increase in complex particle size may result from both reduced negative potential and phenolic compounds serving as bridges to promote protein aggregation, thereby forming larger particle sizes (Xia et al., 2022).

### 3.6. SEM analysis

The microscopic image of the complexes interacting with Que in different concentrations is shown in Fig. 6. It can be seen from the picture that the shape of the SIP was irregular branching and there were many holes in the SIP surface. After adding Que, the SIP surface structure became smooth, indicating that Que loading increased the size of protein particles. The loading of Que increased ζ-potential, possibly due to the rearrangement and enhanced exposure of charged groups upon flavonoid inclusion (Khan et al., 2021). These results suggest that Que can bind with SIP and change protein structure.

### 3.7. Antioxidant activity

The antioxidant activity of the complexes was assessed using DPPH, FRAP, and ·OH radicals scavenging capacity assay kits as shown in Fig. 7. The DPPH radical scavenging capacity increased from 8.76 μg trolox/mL at 17.2 μM to 11.75 μg trolox/mL at 25.8 μM, then fluctuated slightly for 25.8–69.0 μM (Fig. 7A). The FRAP increased from 0.68 mM at 7.2 μM to 0.88 mM at 69.0 μM. The hydroxyl radical scavenging capacity increased from 11.79 U/mL at 7.2 μM to 35.88 U/mL at 69.0 μM. Antioxidant activity increased with higher Que concentrations, suggesting that more quercetin enhances antioxidant capacity. The results indicate that the non-covalent interactions between SIP and Que provide greater radical scavenging than the protein alone (Ma et al., 2022). Additionally, previous research indicates that the combination of polyphenols and proteins resulted in higher antioxidant activity compared to proteins alone (Quan et al., 2019). Zhao et al. also found that adding polyphenols to casein improved its radical scavenging ability, likely due to an increase in free hydroxyl groups (Zhao et al., 2020). These results are consistent with our findings.

### 3.8. Bioaccessibility

Polyphenols often degrade during digestion and they also have low bioavailability, which diminishes their health benefits (Tong et al., 2022). Previous studies have reported that protein polyphenol particles protect blueberry anthocyanins during digestion so that more anthocyanins are transported to the colon for biotransformation. Phenols are

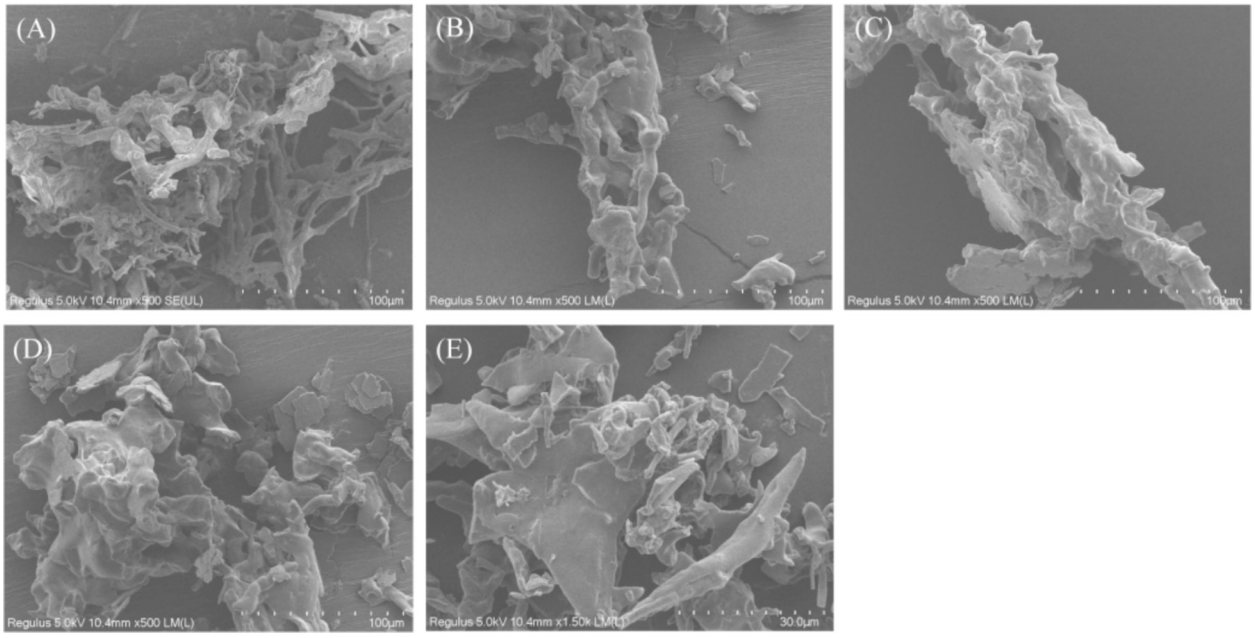


**Fig. 6.** Scanning electron microscope images of SIP and SIP-Que complexes. (A-E) means the Que concentrations are 0, 17.2, 25.8, 34.5, and 69.0 μM.

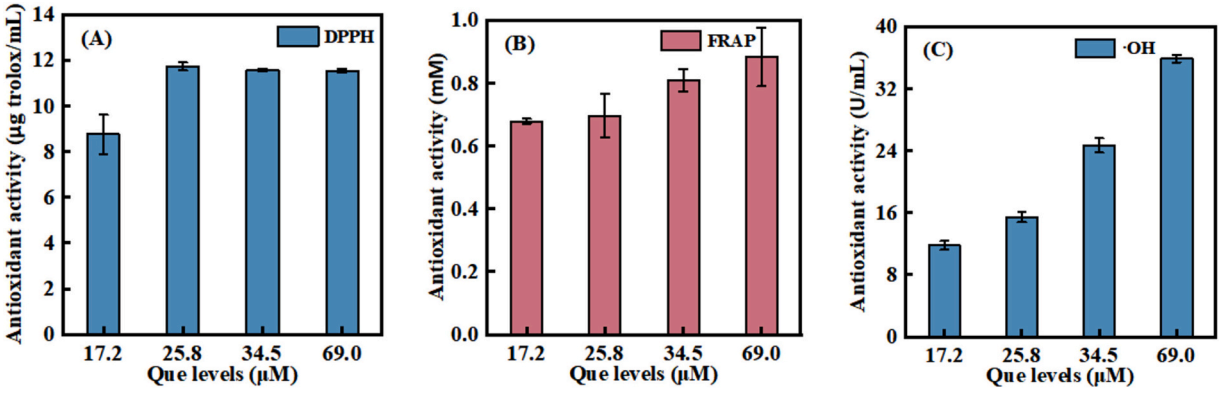


**Fig. 7.** Scavenging ability of DPPH, FRAP and ·OH radicals of SIP-Que complex.

easily dissociated from protein-polyphenol particles during digestion and can be used for subsequent intestinal absorption (bioaccessibility) (Ribnicky et al., 2014). Therefore, enhancing the bioaccessibility of Que is crucial. Fig. 8 shows that the bioaccessibility of Que in the SIP-Que complex was higher than that of free Que, and increased with higher Que concentrations. This improvement may result from the interaction between SIP and Que, which enhances stability and reduces degradation in the gastrointestinal tract. This effect may be due to the hydrophobic internal dissolution of the mixed micelles formed by Que during digestion or its binding to peptide molecules after protein digestion, and the interaction between peptides produced by proteolysis may also contribute to micellization (Chen et al., 2018). Previous studies have shown that loading Que onto zein protein improves its stability during *in vitro* digestion (Lamothe et al., 2014). In Addition, Lamothe et al. found that antioxidant amino acids in proteins, such as cysteine, tyrosine, and tryptophan, interact with polyphenols to enhance their stability during digestion and prevent degradation. Thus, the interaction between SIP and Que can enhance the stability during digestion and improve its bioaccessibility.

## 4. Conclusion

This study explored the interactions between SIP and Que, along with the physicochemical properties of their complexes The non-covalent interactions between SIP and Que are primarily driven by hydrogen bonds and van der Waals forces, and this process is spontaneous. The concentration of Que significantly affected both its loading amount and encapsulation efficiency in SIP. The SIP-Que complexes demonstrated excellent antioxidant properties and enhanced the bioaccessibility of Que. These findings not only help to expand the development and utilization of SIP but also provide a reference for the development of functional food and delivery systems.

## CRediT authorship contribution statement

**Tao Yang:** Writing – original draft, Investigation, Funding acquisition, Data curation. **Shanshan Li:** Investigation. **Wenqin Su:** Investigation. **Kun Pan:** Supervision. **Fei Peng:** Writing – review & editing, Supervision.

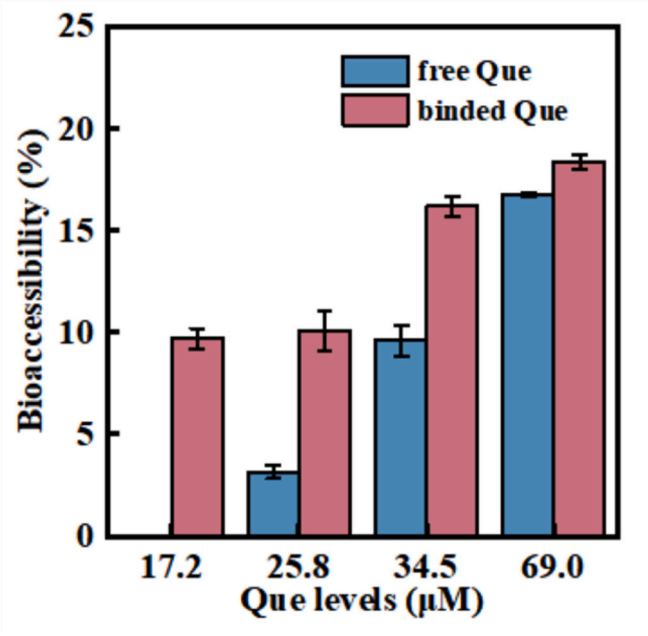


**Fig. 8.** Bioaccessibility of Que in the SIP-Que complexes after *in vitro* simulated digestion.

## Declaration of competing interest

The authors declare that they have no known competing financial interests or personal relationships that could have appeared to influence the work reported in this paper.

## Acknowledgement

This work was supported by the Hainan Province Science and Technology Special Fund (ZDYF2022SHFZ289).

## Data availability

The data that has been used is confidential.

## References

Al-Shabib, N. A., MasoodMalik, J., AjamaluddinAlsenaidy, M. A., TabishAlAjmi, R., .M., Alsenaidy, M. F., et al. (2018). Molecular insight into binding behavior of polyphenol (rutin) with beta lactoglobulin: Spectroscopic, molecular docking and MD simulation studies. *Journal of Molecular Liquids, 269*, 511–520. https://doi.org/10.1016/j.molliq.2018.07.122

Chen, X., McClements, D. J., Zhu, Y., Chen, Y., Zou, L., Liu, W., et al. (2018). Enhancement of the solubility, stability and bioaccessibility of quercetin using protein-based excipient emulsions. *Food Research International, 114*, 30–37. https://doi.org/10.1016/j.foodres.2018.07.062

Cheng, J., Dudu, O. E., Zhang, J., Wang, Y., Meng, L., Wei, W., et al. (2023). Impact of binding interaction modes between whey protein concentrate and quercetin on protein structural and functional characteristics. *Food Hydrocolloids, 142, Article 108787*. https://doi.org/10.1016/j.foodhyd.2023.108787

Cui, Z., Kong, X., Chen, Y., Zhang, C., & Hua, Y. (2014). Effects of rutin incorporation on the physical and oxidative stability of soy protein-stabilized emulsions. *Food Hydrocolloids, 41*, 1–9. https://doi.org/10.1016/j.foodhyd.2014.03.006

Dai, S., Lian, Z., Qi, W., Chen, Y., Tong, X., Tian, T., et al. (2022). Non-covalent interaction of soy protein isolate and catechin: Mechanism and effects on protein conformation. *Food Chemistry, 384*, Article 132507. https://doi.org/10.1016/j.foodchem.2022.132507

Doosti, M., Dorraji, M. S. S., Mousavi, S. N., Rasoulifard, M. H., & Hosseini, S. H. (2019). Enhancing quercetin bioavailability by super paramagnetic starch-based hydrogel grafted with fumaric acid: An in vitro and in vivo study. *Colloids and Surfaces B: Biointerfaces, 183, Article 110487*. https://doi.org/10.1016/j.colsurfb.2019.110487

Ferreira-Santos, P., Nobre, C., Rodrigues, R., Genisheva, Z., Botelho, C., & Teixeira, J. (2024). Extraction of phenolic compounds from grape pomace using ohmic heating: Chemical composition, bioactivity and bioaccessibility. *Food Chemistry, 436, Article 137780*. https://doi.org/10.1016/j.foodchem.2023.137780

Gan, N., Li, Y., Liu, P., Pang, J., Chen, L., Geng, F., et al. (2024). Experimental and computational investigations of zirconium-based metal-organic frameworks for bilirubin adsorption. *Microporous and Mesoporous Materials, 369*, Article 113054. https://doi.org/10.1016/j.micromeso.2024.113054

Ghayour, N., Hosseini, S. M. H., Eskandari, M. H., Esteghlal, S., Nekoei, A.-R., Gahruie, H. H., et al. (2019). Nanoencapsulation of quercetin and curcumin in casein-based delivery systems. *Food Hydrocolloids, 87*, 394–403. https://doi.org/10.1016/j.foodhyd.2018.08.031

Girard, A. L., & Awika, J. M. (2020). Effects of edible plant polyphenols on gluten protein functionality and potential applications of polyphenol–gluten interactions. *Comprehensive Reviews in Food Science and Food Safety, 19*(4), 2164–2199. https://doi.org/10.1111/1541-4337.12572

Günal-Köroğlu, D., Yılmaz, H., Turan, S., & Capanoglu, E. (2022). Exploring the lentil protein and onion skin phenolics interaction by fluorescence quenching method. *Food Bioscience, 50, Article 102000*. https://doi.org/10.1016/j.fbio.2022.102000

Hao, C., Xu, G., Feng, Y., Lu, L., Sun, W., & Sun, R. (2017). Fluorescence quenching study on the interaction of ferroferric oxide nanoparticles with bovine serum albumin. *Spectrochimica Acta Part A: Molecular and Biomolecular Spectroscopy, 184*, 191–197. https://doi.org/10.1016/j.saa.2017.05.004

Hao, L., Sun, J., Pei, M., Zhang, G., Li, C., Li, C., et al. (2022). Impact of non-covalent bound polyphenols on conformational, functional properties and in vitro digestibility of pea protein. *Food Chemistry, 383*, Article 132623. https://doi.org/10.1016/j.foodchem.2022.132623

Huang, Y., Du, H., Kamal, G. M., Cao, Q., & Huang, Q. (2020). Studies on the binding interactions of grass carp (Ctenopharyngodon idella) myosin with Chlorogenic acid and Rosmarinic acid. *Food and Bioprocess Technology, 13*(8), 1421–1434. https://doi.org/10.1007/s11947-020-02483-0

Jiang, F., Du, C., Zhao, N., Jiang, W., Yu, X., & Du, S.-K. (2022). Preparation and characterization of quinoa starch nanoparticles as quercetin carriers. *Food Chemistry, 369, Article 130895*. https://doi.org/10.1016/j.foodchem.2021.130895

Khan, M. A., Zhou, C., Zheng, P., Zhao, M., & Liang, L. (2021). Improving physicochemical stability of quercetin-loaded hollow Zein particles with chitosan/pectin complex coating. *Antioxidants, 10*(9). https://doi.org/10.3390/antiox10091476. Article 9.

Kopjar, M., Buljeta, I., Ćorković, I., Pichler, A., & Šimunović, J. (2022). Adsorption of quercetin on brown rice and almond protein matrices: Effect of quercetin concentration. *Foods, 11(6), Article 793*. https://doi.org/10.3390/foods11060793

Lamothe, S., Azimy, N., Bazinet, L., Couillard, C., & Britten, M. (2014). Interaction of green tea polyphenols with dairy matrices in a simulated gastrointestinal environment. *Food & Function, 5*(10), 2621–2631. https://doi.org/10.1039/c4fo00203b

Liu, J., Li, Y., Zhang, H., Liu, S., Yang, M., Cui, M., et al. (2022). Fabrication, characterization and functional attributes of zein-egg white derived peptides (EWDP)-chitosan ternary nanoparticles for encapsulation of curcumin: Role of EWDP. *Food Chemistry, 372, Article 131266*. https://doi.org/10.1016/j.foodchem.2021.131266

Liu, Z.-W., Zhou, Y.-X., Wang, L.-H., Ye, Z., Liu, L.-J., Cheng, J.-H., et al. (2021). Multi-spectroscopies and molecular docking insights into the interaction mechanism and antioxidant activity of astaxanthin and β-lactoglobulin nanodispersions. *Food Hydrocolloids, 117, Article 106739*. https://doi.org/10.1016/j.foodhyd.2021.106739

Lozano-Pérez, A. A., Rivero, H. C., Hernández, M. D. C. P., Pagán, A., Montalbán, M. G., Víllora, G., et al. (2017). Silk fibroin nanoparticles: Efficient vehicles for the natural antioxidant quercetin. *International Journal of Pharmaceutics, 518*(1–2), 11–19. https://doi.org/10.1016/j.ijpharm.2016.12.046

Ma, C. M., Zhao, J. R., & Wu, X. H. (2022). The non-covalent interacting forces and scavenging activities to three free radicals involved in the caseinate-flavonol (kaempferol and quercetin) complexes. *Journal of Food Measurement and Characterization, 16*(1), 114–125. https://doi.org/10.1007/s11694-021-01157-5

Mirpoor, S. F., Hosseini, S. M. H., & Nekoei, A.-R. (2017). Efficient delivery of quercetin after binding to beta-lactoglobulin followed by formation soft-condensed core-shell nanostructures. *Food Chemistry, 233*, 282–289. https://doi.org/10.1016/j.foodchem.2017.04.126

Qie, X., Chen, W., Zeng, M., Wang, Z., Chen, J., Goff, H. D., et al. (2021). Interaction between β-lactoglobulin and chlorogenic acid and its effect on antioxidant activity and thermal stability. *Food Hydrocolloids, 121, Article 107059*. https://doi.org/10.1016/j.foodhyd.2021.107059

Quan, T. H., Benjakul, S., Sae-leaw, T., Balange, A. K., & Maqsood, S. (2019). Protein–polyphenol conjugates: Antioxidant property, functionalities and their applications. *Trends in Food Science & Technology, 91*, 507–517. https://doi.org/10.1016/j.tifs.2019.07.049

Ribnicky, D. M., Roopchand, D. E., Oren, A., Grace, M., Poulev, A., Lila, M. A., et al. (2014). Effects of a high fat meal matrix and protein complexation on the bioaccessibility of blueberry anthocyanins using the TNO gastrointestinal model (TIM-1). *Food Chemistry, 142*, 349–357. https://doi.org/10.1016/j.foodchem.2013.07.073

Song, G., Li, F., Shi, X., Liu, J., Cheng, Y., Wu, Y., et al. (2024). Characterization of ultrasound-assisted covalent binding interaction between β-lactoglobulin and dicaffeoylquinic acid: Great potential for the curcumin delivery. *Food Chemistry, 441*, Article 138400. https://doi.org/10.1016/j.foodchem.2024.138400

Tong, X., Cao, J., Tian, T., Lyu, B., Miao, L., Lian, Z., et al. (2022). Changes in structure, rheological property and antioxidant activity of soy protein isolate fibrils by ultrasound pretreatment and EGCG. *Food Hydrocolloids, 122, Article 107084*. https://doi.org/10.1016/j.foodhyd.2021.107084

Vasava, H., Singh, R., & Yadav, T. (2022). Characterisation of whey protein–polyphenol conjugates prepared by the noncovalent and covalent methods for their effect on the

functional properties of whey proteins. *International Journal of Dairy Technology, 75* (3), 563–574. https://doi.org/10.1111/1471-0307.12874

Wang, S., Zhu, F., & Kakuda, Y. (2018). Sacha inchi (Plukenetia volubilis L.): Nutritional composition, biological activity, and uses. *Food Chemistry, 265*, 316–328. https://doi.org/10.1016/j.foodchem.2018.05.055

Xia, N., Wang, C., & Zhu, S. (2022). Interaction between pH-shifted ovalbumin and insoluble neohesperidin: Experimental and binding mechanism studies. *Food Chemistry, 390*, Article 133104. https://doi.org/10.1016/j.foodchem.2022.133104

Xiong, J., Chan, Y. H., Rathinasabapathy, T., Grace, M. H., Komarnytsky, S., & Lila, M. A. (2020). Enhanced stability of berry pomace polyphenols delivered in protein-polyphenol aggregate particles to an in vitro gastrointestinal digestion model. *Food Chemistry, 331, Article 127279*. https://doi.org/10.1016/j.foodchem.2020.127279

Yadav, S., Mehrotra, G., Bhartiya, P., Singh, A., & Dutta, P. (2020). Preparation, physicochemical and biological evaluation of quercetin based chitosan-gelatin film for food packaging. *Carbohydrate Polymers, 227, Article 115348*. https://doi.org/10.1016/j.carbpol.2019.115348

Zhang, J., Wu, D., Tang, L., Hu, X., Zeng, Z., Wu, W., et al. (2023). Evaluation of the binding affinity and antioxidant activity of phlorizin to pepsin and trypsin. *Food Science and Human Wellness, 13*(1), 1–16. https://doi.org/10.26599/FSHW.2022.9250033

Zhang, X., Wang, C., Qi, Z., Zhao, R., Wang, C., & Zhang, T. (2022). Pea protein based nanocarriers for lipophilic polyphenols: Spectroscopic analysis, characterization, chemical stability, antioxidant and molecular docking. *Food Research International, 160*, Article 111713. https://doi.org/10.1016/j.foodres.2022.111713

Zhang, Y., Hou, R., Zhu, B., Yin, G., Zhang, J., Zhao, W., et al. (2022). Changes on the conformational and functional properties of soybean protein isolate induced by quercetin. *Frontiers in Nutrition, 9, Article 966750*. https://doi.org/10.3389/fnut.2022.966750

Zhang, Y., & Zhong, Q. (2013). Probing the binding between norbixin and dairy proteins by spectroscopy methods. *Food Chemistry, 139*(1–4), 611–616. https://doi.org/10.1016/j.foodchem.2013.01.073

Zhao, Q., Yu, X., Zhou, C., Yagoub, A. E. A., & Ma, H. (2020). Effects of collagen and casein with phenolic compounds interactions on protein in vitro digestion and antioxidation. *Lwt, 124, Article 109192*. https://doi.org/10.1016/j.lwt.2020.109192

Zheng, J., Xiao, N., Li, Y., Xie, X., & Li, L. (2022). Free radical grafting of whey protein isolate with tea polyphenol: Synthesis and changes in structural and functional properties. *Lwt, 153, Article 112438*. https://doi.org/10.1016/j.lwt.2021.112438